Copper-Binding Motifs: Structural and Theoretical Aspects

by **Amy Kaufman Katz**[a]), **Liat Shimoni-Livny**[a]), **Oshrit Navon**[b]), **Nadav Navon**[b]), **Charles W. Bock**[c]), and **Jenny P. Glusker**[a])*

[a]) The Institute for Cancer Research, Fox Chase Cancer Center, 7701 Burholme Avenue, Philadelphia, PA 19111, USA (tel.: +1-215-728-2220; fax: +1-215-728-2863; e-mail: jp_glusker@fccc.edu)

[b]) The Ben-Gurion University of the Negev, Beer Sheva 84105, Israel

[c]) Philadelphia University, Philadelphia, PA, USA 19144

Dedicated to Professor *Jack D. Dunitz* on the occasion of his 80th birthday

In this paper, we report the results of a study involving the coordination geometries of Cu^{I}, Cu^{II}, and Cu^{III} crystal structures in the *Cambridge Structural Database*, and on Cu binding sites in proteins taken from the *Protein Data Bank*. The motifs used to bind two bridged Cu ions are also described. In addition, we report the results of *ab initio* molecular-orbital calculations performed on a variety of model Cu^{I}/Cu^{II} complexes ($Cu^{I}/Cu^{II} \cdot X_nY_m$ (X, Y = NH_3, SH_2); $n+m=4$; $n=0-4$) to provide data on the structural and energetic changes that occur in isolated complexes when the oxidation state of the Cu ion is changed from II to I while the coordination number is conserved. The use of such simple ligands in these calculations eliminates constraints on the geometric changes that may be imposed by more-complicated ligands.

Introduction. – Copper plays a critical role in the activation of a variety of proteins with functions such as electron transfer, oxygen transport in the body, and oxygen insertion into a substrate [1][2]. On the other hand, Cu can be toxic (even at low concentrations) when free within a cell. This toxicity is avoided by restricting the movement of Cu ions. So-called chaperone proteins, such as Atx1 (Cu chaperone for the yeast P-type ATPase cation transporter) [3] and CCS (Cu chaperone for superoxide dismutase) [4], guide Cu ions to their appropriate locations in the cell. In this way, they protect the cell by keeping the concentration of free Cu ions extremely low (less than one free Cu ion per cell) [5]. In this article, we examine the ways in which Cu ions are bound in both large and small molecular systems.

Both Cu^{I} and Cu^{II} are very effective at binding organic molecules [6], in part due to their relatively high electron affinity [7]. The nearly equal tendency of Cu^{I} and Cu^{II} to form organic complexes makes the Cu^{I}/Cu^{II} couple [8] a very useful and adaptable tool for biological systems. Since the reduced state of Cu is more stable than its oxidized state, Cu^{II} tends to abstract electrons from a substrate, thereby becoming Cu^{I}. Cu^{II} Complexes show a *Jahn–Teller* effect [9–12] in which distortion of the Cu^{II}-coordination polyhedron occurs as a result of energy-level splitting that reduces degeneracy and provides additional stabilization. In Cu^{II} complexes that show this effect, ligand–Cu^{II} distances are elongated or compressed along a particular direction.

Cu Proteins can be broadly classified into one of three types based on their spectral properties [8][13][14]:

a) Type 1 blue Cu proteins have a visible absorption band near 600 nm. Their intense blue coloration is characteristic of the oxidized Cu^{II} state and attributed to a

cysteine S → Cu charge transfer. Type 1 Cu enzymes usually contain a four-coordinated (distorted tetrahedral) Cu ion, although a coordination number of five is found in the azurins [14][15]. There is a well-defined structural motif at the active site consisting of the arrangement $Cu^{I}/Cu^{II}(His)_2CysX$, where X is normally Met (although, in stellacyanin, it is Gln [16]). Examples of the $Cu^{I}/Cu^{II}(His)_2CysX$ motif can be found in pseudoazurin [17], rusticyanin [18], plastocyanin [19], and amicyanin [20][21]. Interestingly, it has been shown that replacing a Cu^{I} ion in type 1 proteins with Cu^{II} causes minimal structural change. This feature allows for low activation barriers for redox processes and facilitates rapid electron-transfer rates [14][22][23]. The geometry of the ligands surrounding a type 1 Cu ion in proteins is, presumably, intermediate between preferred ligand dispositions for the two different oxidation states of Cu.

b) Type 2 Cu proteins (low-blue Cu proteins with an absorption band at 350–420 nm) have a less-intense color than type 1 proteins at normal concentrations. These proteins include superoxide dismutase (which converts the harmful superoxide radical to O_2 and H_2O_2, *i.e.*, dismutates it) [24], galactose oxidase (which reduces O_2 to H_2O_2, thereby oxidizing galactose to an aldehyde) [25][26], and amine oxidase (which oxidatively deaminates primary amines to give aldehydes) [27]. The Cu in these type 2 proteins is usually found in a square planar or tetragonal coordination and catalytic oxidation of substrate (after binding) is facilitated by vacant coordination sites around the Cu ion.

c) Type 3 Cu proteins are characterized by an antiferromagnetically-coupled pair of Cu ions and a strong absorption band near 330 nm. Examples include the invertebrate protein hemocyanin [28], which is involved in oxygen transport, and tyrosinase [29], which is a monooxygenase that hydroxylates monophenols and oxidizes diphenols to quinones. No crystal structure is yet available for tyrosinase.

The nature and geometry of the ligand (substrate) atoms around the Cu ions allow a protein to control the extent to which reactions are catalyzed. This control is, in part, effected by the nature (softer or harder) of the binding groups [30]. In this paper, we report the results of a study of the coordination geometries of Cu^{I}, Cu^{II}, and Cu^{III} crystal structures in the *Cambridge Structural Database* (*CSD*) [31], and on Cu binding sites in proteins taken from the *Protein Data Bank* (*PDB*) [32]. In addition, we report the results of *ab initio* molecular-orbital calculations that were performed on a variety of model Cu^{I}/Cu^{II} complexes $[Cu^{I}/Cu^{II} \cdot X_nY_m$ (X, Y = NH_3, SH_2; $n+m=4$; $n=0-4]$ to provide data on the structural and energetic changes that occur in isolated complexes when the oxidation state of the Cu ion is changed from II to I while the coordination number is conserved. The use of such simple ligands in these studies eliminates constraints on geometric changes that may be imposed by more complicated ligands, giving results relevant to geometric changes that occur in the vicinity of a Cu center in a redox process.

Experimental. – 1. *Structural Analyses.* The coordination geometries of Cu^{I}, Cu^{II}, and Cu^{III} ions were probed by use of the atomic coordinates of crystal structures containing these cations in the *CSD* (2002 release) [31]. This database contains three-dimensional parameters for atoms in a wide variety of Cu complexes; the diversity of reasons behind the choices of these complexes for study is sufficiently wide for us to derive hints about the binding preferences of Cu from them. The search for all published crystal structures containing Cu ions was performed with the program QUEST3D, which is part of the database. A master file was created of three-dimensional coordinates and bibliographic references for the crystal structures found by this search. Some

crystal structures were eliminated from the analysis because they contained disorder and/or the crystallographic *R* factor was high (>0.10).

The master file of Cu-containing compounds so obtained was separated into groups according to the oxidation states and coordination numbers of the Cu. The coordination number of the Cu ion was evaluated by inspection of its surroundings in the crystal structure with the computer graphics program ICRVIEW [33]. It can also be found from the chemical formula drawn by the software provided within the *CSD* program system. The oxidation state of Cu was generally taken directly from the chemical formula given in the database or in the title of the article.

In a similar way, the *PDB* [32] was accessed for the analysis of protein structures. Each Cu-containing-protein crystal structure was viewed on our computer-graphics system and the metal-ion environment was examined [33].

2. Ab Initio *Molecular-Orbital Study. Ab initio* molecular-orbital optimizations (with relativistic corrections, as described below) were performed on a variety of Cu complexes by means of second-order *Møller-Plesset* (MP2) perturbation theory with the GAUSSIAN 94 series of programs [34]. These calculations were performed on the *Cray* computer at the *National Cancer Institute*, Frederick, MD and on a variety of DEC alpha and SGI workstations in Philadelphia. The 6-311 ++ G** and LANL2DZ basis sets were employed. The LANL2DZ basis set uses the *Dunning–Huzinaga* full double zeta (D95) basis set on atoms in the first row and the Los Alamos effective core potential plus DZ on Na–Bi [35–38]; we augmented this basis set with additional *d*-functions on all the heavy atoms [39]. This computational method incorporates the major relativistic effects (that is, *Darwin* and mass-velocity terms) by fitting the atomic pseudopotential parameters to relativistic all-electron *Hartree-Fock* (HF) atomic wave functions [35–37].

Unless otherwise noted, optimizations were carried out with no symmetry constraints, to reduce the likelihood of the final structure being a transition state rather than a local minimum on the potential-energy surface (PES). In many cases, the OPT = TIGHT option in GAUSSIAN 94 was used to tighten the cutoffs on the residual forces and displacements used as criteria for convergence of the optimization [34]. For the smaller complexes, frequency analyses were performed to confirm that the calculated structures were local minima in the PESs. The wave functions of the Cu complexes were analyzed by means of natural-bond-orbital (NBO) analyses [40–42]; the *Reed/Weinhold* NAO/NBO analysis package is part of GAUSSIAN 94 [34].

Results. – CSD *Study: Structural Analysis.* Since O, N, and S are the most-significant ligand atoms in biological systems, the analysis described here is restricted to those Cu complexes in the *CSD* that are liganded to *exclusively* these atoms. A total of 5813 crystal structures in the *CSD* that contain Cu ions were included in this study; other structures that showed disorder or had a high *R* value were eliminated by our input to the program. Of the 5813 crystal structures we included, *ca.* 89% involve Cu^{II}, showing that this is, by far, the predominant oxidation state of Cu in structures listed in the *CSD*; Cu^{I} and Cu^{III} are found in only 10% and 1%, respectively, of the entries in this database.

The percentage distributions of the coordination numbers for Cu^{I}, Cu^{II}, and Cu^{III}, which range from 2–8, are shown in *Fig. 1*. The most-common coordination number for both Cu^{I} (614 entries) and Cu^{III} (28 entries) is 4, whereas coordination numbers 4 and 5 are about equally prevalent for Cu^{II} (5171 entries). Of those Cu^{I} complexes that have a coordination number of 4, most have an inner sphere composed of four N-atoms, while only a few have four S-atoms in the inner sphere. It should be noted that the distribution in *Fig. 1* does not change significantly when the *CSD* search is *enlarged* to include Cu ions liganded to atoms other than O-, N-, or S-atoms, although the range of coordination numbers increases to include 9 (two entries) and 10 (four entries). No Cu compounds with coordination numbers higher than 10 were found in this *CSD* search, regardless of ligand identity.

The ligand-atom-binding preferences of the Cu complexes in the *CSD* are shown as relative proportions of O, N, and S in *Fig. 2* with triangular plots [43]. In these plots, each corner of the equilateral triangle represents 100% binding preference to one of

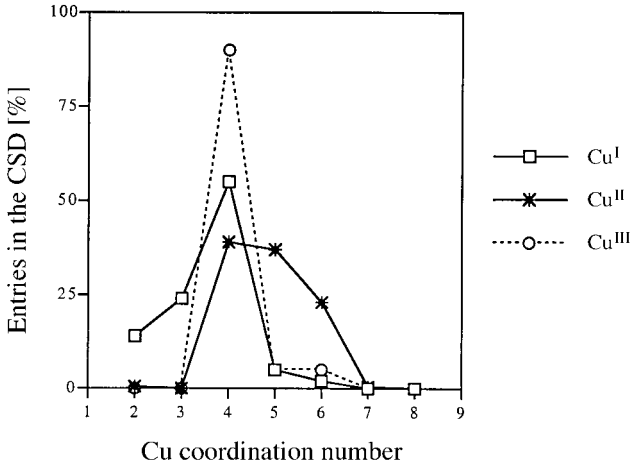

Fig. 1. *Relative frequency of entries in the* CSD *for structures of each coordination number for* Cu^{I}, Cu^{II}, *and* Cu^{III}

the three elements, O, N, and S, which are the most-significant metal-bound ligand atoms in biological systems. The most-common coordination states are indicated by filled circles. As can be seen in *Fig. 2*, Cu^{I} (which is relatively 'soft' [30]) is found most commonly in crystal structures with N and S (nearer to N) as ligand atoms. On the other hand, Cu^{II} (which is relatively 'hard' [30]), with coordination number 4, 5, or 6, is found more commonly with O and N as ligand atoms, *i.e.*, along the N–O side of the triangle in *Fig. 2*. Cu^{III} Complexes generally have a coordination of four S-atoms (64% of all the Cu^{III} compounds in the *CSD*).

Many enzymes make use of metal-ion-bound H_2O molecules in their catalytic mechanisms. In Cu enzymes, H_2O is often the product of reduction of an oxygen-containing species [14]. We analyzed the propensity of Cu to bind H_2O molecules in crystal structures. It was found that 1170 of the 5813 Cu complexes included in this study had at least one H_2O in the inner coordination spheres; of these, 1168 involve Cu^{II} and only two involve Cu^{I} (refcodes BIZBUH and JUXWAA). A list of the number of H_2O molecules bound *vs.* the coordination number is given in *Table 1*. The main entry in this table is Cu^{II} with a coordination number of 5, which has one H_2O molecule in the inner shell (609 entries, 52% of all the Cu^{II}-H_2O interactions). The next highest is Cu^{II} with a coordination number of 6, which has two H_2O molecules in the first shell (228 entries, 19%). It should be noted that many other divalent metal ions commonly bind H_2O [43][44]. For a metal ion that readily binds H_2O, one might expect that there would be a tendency for the inner coordination shell to be filled with H_2O molecules, and the greater this tendency, the greater the inference of the attraction of that metal ion for H_2O. Therefore, we compared the incidence in the *CSD* of $M[H_2O]_6^{2+}$ (*i.e.*, six H_2O molecules in the innermost shell) for Cu, Ni, Zn, and Mg; Mg^{II} was included because it is known to bind H_2O well [45]. The resulting percentages, shown in *Table 2*, clearly suggest that Cu^{II}, Zn^{II}, and Ni^{II} do not attract H_2O as well as Mg^{II} does. In biochemical systems, however, the important consideration is the balance between H_2O molecules and other ligands that are in the first coordination shell for a given

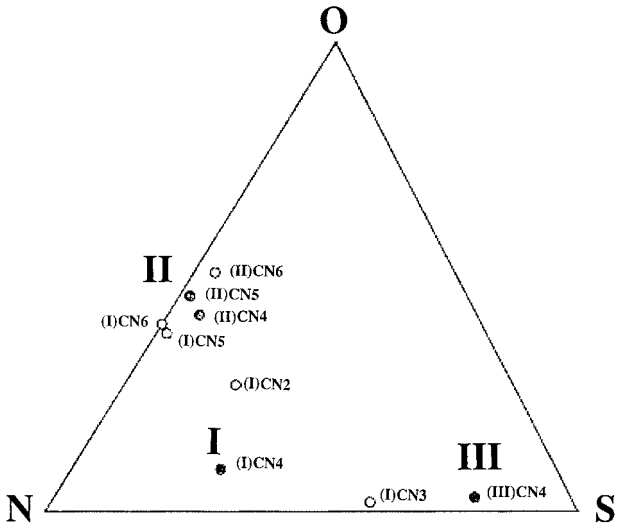

Fig. 2. *Distribution of N, O, and S ligands in Cu complexes as a function of Cu oxidation state* (in parentheses) *and coordination number* (CN). Categories having fewer than three entries are not included. The commonly encountered forms (see *Fig. 1*), indicated by filled circles, are Cu^{I} coordination number 4, and Cu^{II} coordination numbers 4 and 5. Less common is Cu^{III} coordination number 4.

coordination number. Divalent Cu, Zn, and Ni ions appear to be quite good at binding fewer than six H_2O molecules in the innermost shell, which suggests that these ions have a strong preference for other liganding atoms in addition to the H_2O molecules. This is quite unlike Mg, which is surrounded by six H_2O molecules in over 40% of its aquated complexes in the *CSD* [45]. The binding of a combination of H_2O plus other ligands facilitates catalysis in which substrates often displace metal ion-bound water molecules.

Table 1. *Number of H_2O Molecules as a Function of Coordination Number for Copper Complexes.* Taken from the *CSD* (version April, 2002). Total number of Cu complexes containing at least one H_2O molecule = 1170.

Number of H_2O molecules	Coordination number				
	3	4	5	6	7
1	1	30	609	88	
2		37	68	228	4
3			25	18	
4		2	4	42	
5				2	
6				12	

The geometry of 4-coordinated Cu-ion complexes depends on the oxidation state: d^{10} Cu^{I} complexes show a strong tendency to have a tetrahedral arrangement of ligands, whereas the d^9 Cu^{II} and d^8 Cu^{III} complexes show a greater tendency to have a square-planar arrangement of ligands. These results are expected based on ligand-field theory [40]. Interligand interactions, however, can cause substantial distortions in these

Table 2. *Attraction of Selected Metal Ions for Water.* Relative incidence of $M[H_2O]_i^{2+}$.

Metal ion	$i<6$ [%] [a])	$i=6$ [%] [a])
Cu^{2+}	31	3
Zn^{2+}	37	5
Ni^{2+}	28	7
Mg^{2+}	57	42

[a]) Among all entries for that metal ion with coordination number 6.

complexes. For example, the average sum of the six R–Cu–R angles in the 4-coordinated *homoleptic* $Cu^{II}R_4$ complexes found in the *CSD* is 704(6)°, a significant deviation from 657° for regular tetrahedral geometry, and closer to 720°, the value for a square-planar arrangement. By contrast, the average sum of the six angles for the 4-coordinated Cu^{I} complexes found in the *CSD* is 658(8)°, very close to the value for a regular tetrahedron. In the 6-coordinated Cu^{I} and Cu^{II} complexes found in our *CSD* search, the average sums of the angles are 1605°(158) and 1602°(17), respectively, not significantly different from the regular octahedral angle sum of 1620°.

The average Cu–X (X = N, O, S) distances for the complexes found in the *CSD* are shown in *Table 3* as a function of the oxidation state and coordination number of the Cu ion. As found for metal ions in general [46], higher oxidation numbers and lower coordination numbers lead to shorter metal-ion ··· ligand distances. An analysis of the Cu^{II}–X (X = N, O, S) distances in the 6-coordinate Cu complexes shows two axially-disposed ligands that are different in length from the four equatorially-disposed ligands; this is a consequence of the *Jahn–Teller* effect [9–12], and is illustrated for $Cu[H_2O]_6^{2+}$ complexes in *Table 4*. Our *CSD* search shows that O-atoms have a strong preference for the axial position, while N-atoms have a strong preference for the equatorial position. We also examined polynuclear Cu complexes, since type 3 Cu proteins have a binuclear Cu center. The Cu ··· Cu distance in these proteins is on the order of 2.6 Å, but this can expand to accommodate a bridging ligand. In an analysis of such structures in the *CSD*, we found an average Cu ··· Cu distance of 2.68 Å (1138 entries); this was reduced to 2.65 Å (1065 entries) when structures with Cu ··· Cu greater than 2.8 Å were eliminated.

PDB *Study: Active Sites of Cu-Containing Proteins.* For comparison, the binding modes of Cu ions in proteins were also studied. A search of the *PDB* (January, 2003) [32] revealed 358 Cu-containing protein crystal structures. Structures of 36 different types of proteins were represented. These analyses involved various experimental conditions and several different mutants. The Cu ions in proteins of type 1 usually bind two His, one Cys, and one Met residue [$(His)_2$CysMet] to form a distorted tetrahedral geometry around the Cu ion. This is shown in *Fig. 3* for azurin [15] in which three ligands (His46, His117, and Cys112) bind strongly in an approximately planar arrangement. Two axial ligands (Met and a glycine main-chain carbonyl group) are more distant from the metal ion. This binding site is found to be located within 6–10 Å of the enzyme surface. One of the His residues, denoted His_A, serves as a conduit between the Cu ion and the protein surface and is solvent accessible, while the second, denoted His_B, is further away from the protein surface and is not accessible to solvent.

Table 3. *Average Cu–X* (X = N, O, S) *Bond Distances as a Function of Cu Oxidation State and Coordination Number.* Taken from crystal structures in the *CSD*.

Coordination number	Bond distance [Å][a])		
	Cu–N	Cu–O	Cu–S
Cu^{I}			
2	1.90(6)	1.84(2)	2.17(2)
3	1.98(10)	2.14(7)	2.26(4)
4	2.04(8)	2.05(18)	2.33(7)
5	2.07(12)	2.09(21)	2.33(1)
6	2.07(10)	2.26(23)	–
Cu^{II}			
2	1.86(1)	–	2.15(10)
3	–	–	–
4	1.98(5)	1.93(3)	2.28(4)
5	2.03(9)	2.07(19)	2.43(20)
6[b])	2.01(3)/2.40(15)	1.97(4)/2.47(14)	2.38(6)/2.83(18)
7	–	2.15(16)	–
Cu^{III}			
4	1.85(4)	1.81(1)	2.22(5)
5	2.08(15)	2.03(2)	[c])

[a]) Estimated standard deviation for the *CSD* bond lengths in parentheses. [b]) Two distinct categories of bond distances as a result of the *Jahn–Teller* effect. [c]) Single entries not listed.

Table 4. Jahn–Teller *Effect in* $Cu[H_2O]_6^{2+}$

CSD Refcode	Cu–O Bond length [Å]	
	Equatorial	Axial
BENSCU	1.956, 1.979	2.260
BENSCU	1.962, 1.985	2.264
CAMSCU	1.967, 1.971, 2.022, 2.054	2.166, 2.224
CDSRCA10	1.973, 1.986	2.321
CUMALH01	1.949, 1.993	2.408
DODDOP	1.939, 1.997	2.412
DUWWEX	1.973, 1.986	2.321
KAYWAI	1.925, 1.991	2.332
NERKUQ	1.968	2.376
SAFLAM01	1.957, 1.972	2.321
SIYZIJ	1.945, 1.953	2.423
TOLSCV	1.953, 1.954	2.385

In type 1 Cu proteins, His_A generally binds to the Cu ion through Nδ1, while Nε2 of the same His residue interacts with a H_2O molecule. This is surprising because it is more common for a His residue to bind metal ions through Nε2 than Nδ1 [47][48]. Spectroscopic studies have shown, however, that binding a metal ion through Nδ1 is energetically more favorable in basic aqueous solution [49–52]. His_B also binds the Cu ion through Nδ1, but the Nε2 N-atom interacts with a carbonyl O-atom from either the protein backbone or an amino acid side chain such as Asn.

Although the Cu-binding geometry does not depend significantly on the Cu oxidation state, it can be affected by changes in the pH of the environment. For

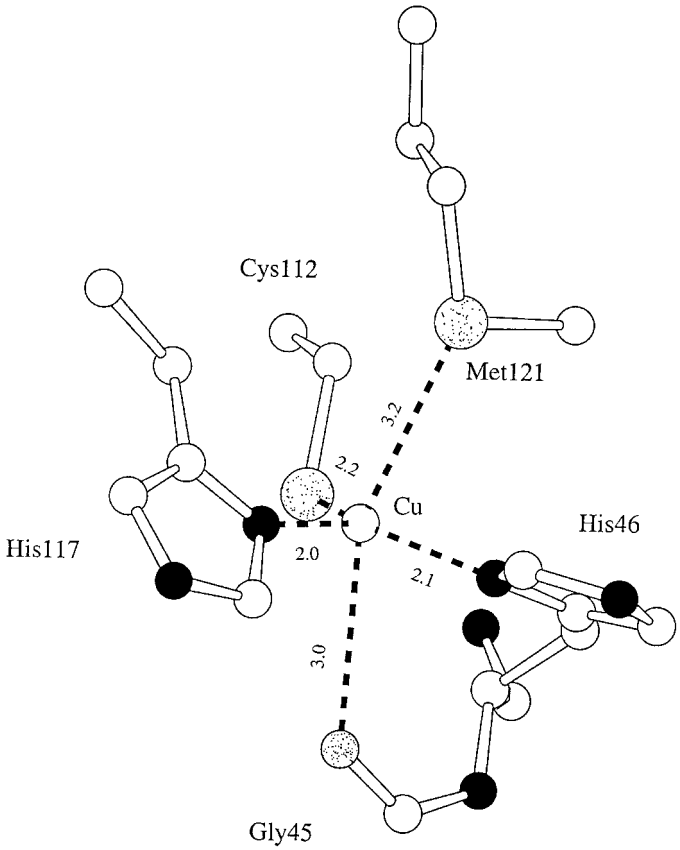

Fig. 3. *Crystal structure of azurin* (5AZU) [15] *showing the type 1 like structure.* Distances are in Å. In this and the following molecular diagrams, N-atoms are filled circles, O- and S-atoms (S-atoms being larger) are speckled and C-atoms are white.

example, in one of the crystal structures of pseudoazurin [53], His_A is further away from the Cu ion at pH 4.4 than at pH 7.8. In another example, the His_A residue in the crystal structure of plastocyanin [54] is fully dissociated from the Cu complex at pH 3.8. This reduces the coordination number to 3, and the Cu ion loses its ability to take part in an electron-transport process. A general two-dimensional schematic diagram that illustrates the interactions taking place in type 1 Cu proteins is shown in *Fig. 4*.

While type 1 and 2 Cu proteins both have His residues at the active site, the identity of the additional ligands to Cu determines the function of the Cu site. In type 2 proteins, the His residue binds the Cu ion through either Nδ1 or Nε2. The other His N-atom interacts with a carbonyl O-atom from the protein backbone, amino acid side chain, or another metal ion such as Zn^{2+} (*e.g.*, in superoxide dismutase).

The known type 2 Cu proteins such as superoxide dismutase [55] and galactose oxidase [25] have more-diverse ligand combinations than do type 1 Cu proteins. Unlike type 1 proteins, where the ligand atoms to Cu are generally N and S, in type 2 proteins,

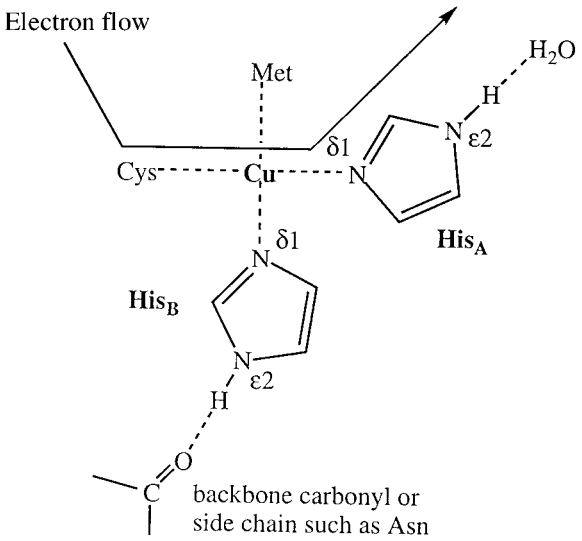

Fig. 4. *Schematic diagram of the flow of electrons in type 1 Cu proteins*

the ligand atoms are usually N and O. In the two examples of type 2 Cu proteins given in *Table 5*, the Cu ion has a coordination number of 5. The Cu ion in superoxide dismutase is ligated to $(His)_4H_2O$, while galactose oxidase is ligated to $(His)_2(Tyr)_2(H_2O)$ or $(His)_2(Tyr)_2$ (coordination number 4), depending on the pH of the environment.

Hemocyanin [28], shown in *Fig. 5*, provides an example of a type 3 enzyme. It is a binuclear Cu complex in which the metal ions can accommodate a bridging ligand. Combinations of types of Cu in enzymes such as laccase [56] and ascorbate oxidase [57] are found. The Cu ions are generally held in place by three His side chains each, while the bridging atoms are generally O- or S-atoms.

In contrast to these enzyme-active-site configurations, the chaperone proteins, such as HAH1, bind Cu ions by way of four Cys ligands, as shown in *Fig. 6* [3]. The arrangement is tetrahedral, but presumably very efficient as it is necessary to prevent free Cu ions from accumulating in any living cell.

Ab initio *Molecular-Orbital Study: Calculated Geometric and Electronic Properties of Gas-Phase Cu Complexes.* In our molecular-orbital studies, we initially optimized the complexes $Cu^I \cdot NH_3$ and $Cu^{II} \cdot NH_3$ at the MP2(FULL)/6-311++G** computational level to compare with the corresponding results for $Cu^I \cdot OH_2$ and $Cu^{II} \cdot OH_2$ [58]. Symmetry was enforced during these calculations. As expected, the Cu–X (X = N, O) distances contract as the oxidation state is changed from I to II, and the effect is more dramatic in monohydrates than in the monoamines. More negative charge is transferred to the Cu ion when the ligand is NH_3 than when it is H_2O, and a significant portion of this additional charge goes into the 4*s* Cu orbital. Nevertheless, the binding in both $Cu^I/Cu^{II} \cdot NH_3$ and $Cu^I/Cu^{II} \cdot OH_2$ complexes is primarily electrostatic. In *Table 6* we compare the calculated binding energies of $Cu^I/Cu^{II} \cdot NH_3$ with those of $Cu^I/Cu^{II} \cdot OH_2$ [58]. The NH_3 binding enthalpies are found to be considerably more negative than the H_2O binding enthalpies [59]. The calculated N–H and Cu–N

Table 5. *Metal Coordination in Copper Proteins*

Copper protein type/ coordination	Groups involved	Examples
Type 1		
N_2S_2	$(His)_2$ Cys Met	Plastocyanin, pseudoazurin, amicyanin, rusticyanin, plantacyanin, auracyanin, cucumber basic protein
N_2SO	$(His)_2$ Cys Gln	Stellacyanin
N_2S_2O	$(His)_2$ Cys Met carbonyl	Azurin
Type 2		
N_4	$(His)_4$	Cu,Zn Superoxide dismutase
N_4O	$(His)_4$ (H_2O)	Cu,Zn Superoxide dismutase
N_3O_2	$(His)_3$ $(H_2O)_2$	Cu amine oxidase
$N_2O_2(O,S)$	$(His)_2$ $(Tyr)_2$ (H_2O/substrate)	Galactose oxidase
$N_2(O,S)$	$(His)_2$ (solvent/Met)	Peptidylglycine monooxygenase
N_3	$(His)_3$	Peptidylglycine monooxygenase
Type 3		
$N_3(O,S)$	$(His)_3$ Cu (ligand) Cu $(His)_3$	Hemocyanin
Types 1 + 2		
N_2S_2 (Type 1)	$(His)_2$ Cys Met	Nitrite reductase
$N_3(O,S)$ (Type 2)	$(His)_3$ (H_2O/OH)	Nitrite reductase
Types 1, 2, + 3		
N_2S_2 (Type 1)	$(His)_2$ Cys Met	Ascorbate oxidase[a])
$N_2(O,S)$ (Type 2)	$(His)_2$ (H_2O/OH)	Ascorbate oxidase[a])
$N_3(O,S)$ (Type 3)	$(His)_3$ Cu (H_2O/OH) Cu $(His)_3$	Ascorbate oxidase[a])
$N_2S(O,S)$ (Type 1)	$(His)_2$ Cys Leu	Laccase[a])
$N_2(O,S)$ (Type 2)	$(His)_2$ (H_2O/OH)	Laccase[a])
$N_3(O,S)$ (Type 3)	$(His)_3$ Cu (H_2O/OH) Cu $(His)_3$	Laccase[a])

[a]) Protein types 2 and 3 can make up a trinuclear center

stretching frequencies of $Cu^I/Cu^{II} \cdot NH_3$ and ammonia show that Cu^{II} has a much greater impact on the N–H stretching frequency in these complexes than does Cu^I, in accord with the shorter Cu–N distance and more-negative binding energy with the divalent ion. Several attempts to locate a local minimum on the PES of $Cu^{III} \cdot OH_2$ failed; the complex consistently decomposed into Cu^{II} and H_2O^+ [60]. By contrast, several other first-row trivalent transition metal ion monohydrates, *e.g.*, $V^{III} \cdot OH_2$ and $Fe^{III} \cdot OH_2$, have been shown to be local minima on their respective PESs [61] [62] at the MP2(FULL)/6-311 + + G** computational level. We expect that additional H_2O molecules or other ligands in the inner coordination shell might eliminate the problem we found for $Cu^{III} \cdot OH_2$.

The ligand-atom preferences for Cu-ion complexes can be investigated relative to those for other metal-ion complexes by calculating the energetics of the transfer reactions, $Cu^I/Cu^{II} \cdot L_1 + M^I/M^{II} \cdot L_2 \rightarrow Cu^I/Cu^{II} \cdot L_2 + M^I/M^{II} \cdot L_1$. The enthalpy and *Gibbs* free energy changes for the competition of NH_3 and H_2O for Mg and Cu ions (monovalent and divalent) show that Cu^I and, particularly, Cu^{II}, have a significant

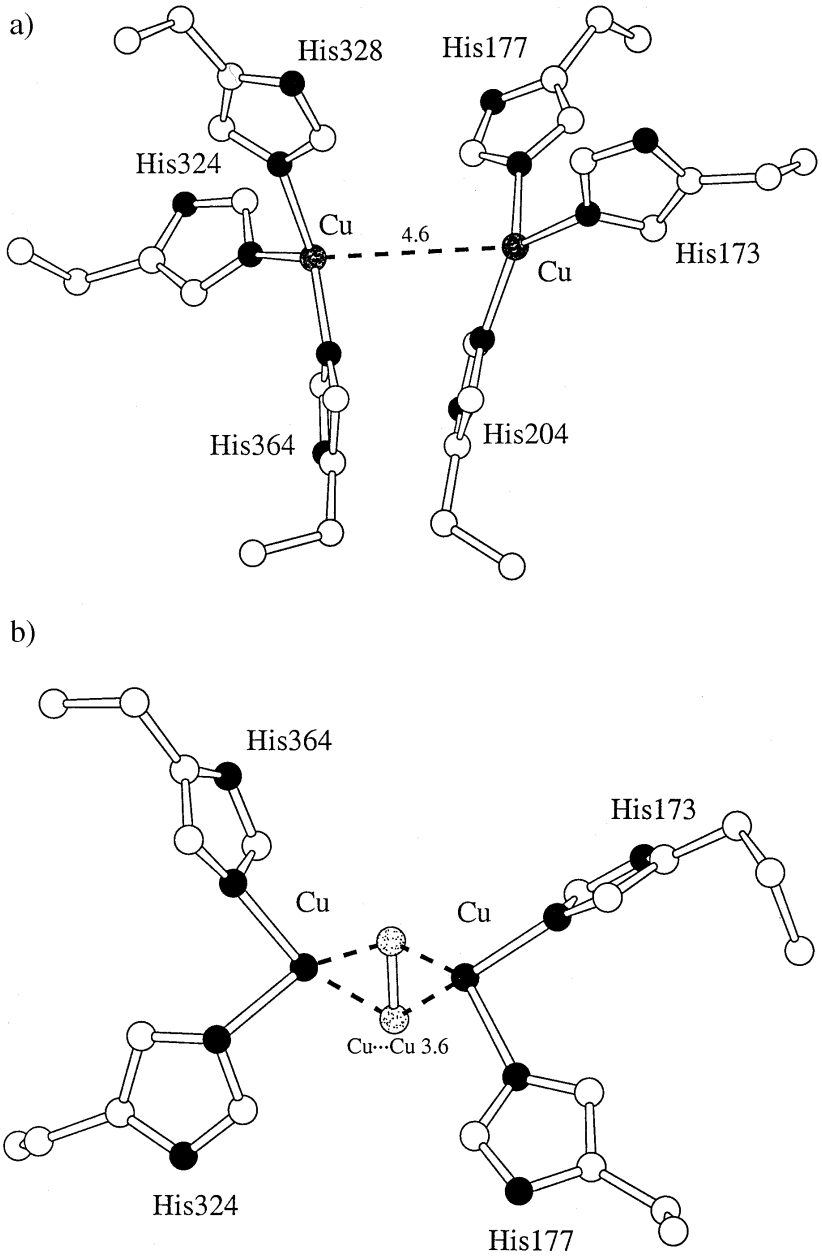

Fig. 5. *The crystal structure of hemocyanin showing* a) *the Cu–Cu distance of 4.6 Å* (1LLA) *and* b) *the Cu–Cu distance reduced to 3.6 Å when O_2 binds* (1NOL) [28]

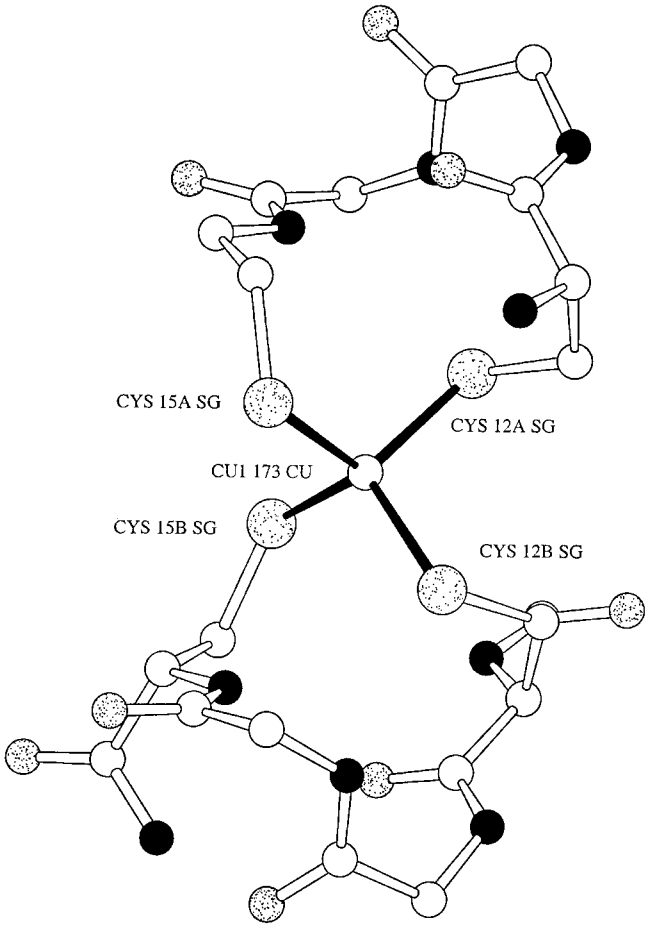

Fig. 6. *The crystal structure of Cu protein HAH1* (Atx1, refcode 1FEE) [5], *a Cu chaperone protein, showing four Cys binding the Cu ions*

Table 6. *Calculated Binding Enthalpies of* $Cu^{I}/Cu^{II} \cdot NH_3$ *and* $Cu^{I}/Cu^{II} \bullet OH_2$ *at the MP2(FULL)/6-311++G** Computational Level*

Reaction	ΔH°_{298}
$Cu^{I} + H_2O \rightarrow Cu^{I}\,OH_2$	−37.7
$Cu^{II} + H_2O \rightarrow Cu^{II} \cdot OH_2$	−102.3
$Cu^{I} + NH_3 \rightarrow Cu^{I} \cdot NH_3$	−55.1
$Cu^{II} + NH_3 \rightarrow Cu^{II} \cdot NH_3$	−134.2

energetic preference for an NH_3 over a H_2O ligand relative to the corresponding Mg ions.

To follow the detailed geometric and electronic changes that take place when a larger Cu^{II} complex is reduced to the corresponding Cu^{I} complex (in a process in which

Table 7. *NPA Charges and Natural Electron Configurations of* $Cu^{I}/Cu^{II} \cdot X_nY_m$ (X, Y = NH_3, SH_2, $n+m=4$, $n=0-4$)

Structure	Oxidation state	NPA Cu Charge	NPA Charge on liganded atoms	Natural electron configuration of Cu^{I}/Cu^{II} (SCF density)
$Cu \cdot (NH_3)_4$	I	+0.869	N: −1.163	[core]4s(0.14)3d(9.97)5p(0.02)
	II	+1.652	N: −1.229	[core]4s(0.25)3d(9.07)4p(0.01)5p(0.01)
$Cu \cdot (NH_3)_3SH_2$	I	+0.839	N: −1.168, −1.169, −1.170	[core]4s(0.17)3d(9.97)5p(0.02)
			S: −0.257	
	II	+1.604	N: −1.234, −1.238, −1.235	[core]4s(0.29)3d(9.07)4p(0.01)5p(0.01)
			S: −0.272	
$Cu \cdot (NH_3)_2(SH_2)_2$	I	+0.802	N: −1.173, −1.178	[core]4s(0.20)3d(9.97)5p(0.02)
			S: −0.259, −0.254	
	II	+1.537	N: −1.240, −1.242	[core]4s(0.34)3d(9.07)4p(0.04)5p(0.01)5p(0.01)
			S: −0.269, −0.262	
$Cu \cdot NH_3(SH_2)_3$	I	+0.759	N: −1.180	[core]4s(0.24)3d(9.97)5p(0.01)6p(0.03)
			S: −0.255, −0.261, −0.254	
	II	+1.467	N: −1.245	[core]4s(0.38)3d(9.08)4p(0.06)4d(0.01)5p(0.01)
			S: −0.265, −0.271, −0.263	
$Cu \cdot (SH_2)_4$	I	+0.710	S: −0.256	[core]4s(0.24)3d(9.97)5p(0.01)6p(0.03)
	II	+1.382	S: −0.265	[core]4s(0.43)3d(9.09)4p(0.08)4d(0.01)5p(0.01)

the coordination number is conserved), *ab initio* molecular-orbital calculations were performed on a variety of four-coordinate Cu complexes of the form $Cu^{I}/Cu^{II} \cdot X_mY_n$ (X, Y = NH_3, SH_2; $n+m=4$, $n=0-4$). The MP2/LANL2DZ + *d* optimized structures of these complexes with different ligand combinations are shown schematically in *Fig. 7*; the NPA charges and natural electron configurations are given in *Table 7*. The geometric parameters of the complexes are listed in *Table 7*. It is clear from *Table 7* that the bonding in these complexes is primarily electrostatic, although some charge is transferred from the ligands to the Cu ion in all cases. More charge is transferred to the Cu ions as the number of (less-electronegative) liganding S-atoms increases. In each of the five pairs of complexes, the charge transferred to the Cu ion in the Cu^{II} $3d^9$ complex is consistently more than double the charge transferred to the corresponding Cu^{I} $3d^{10}$ complex.

During the reduction process, $Cu^{II} \cdot X_nY_m + e^- \rightarrow Cu^{I} \cdot X_nY_m$, a significant portion (0.78 – 0.67e) of the electron gained by the $Cu^{I} \cdot X_nY_m$ complex goes directly into lowering the effective positive charge on the Cu ion (see *Table 7*). The population of the Cu 3d orbital increases (0.90 – 0.88e), but there is a concomitant decrease in the

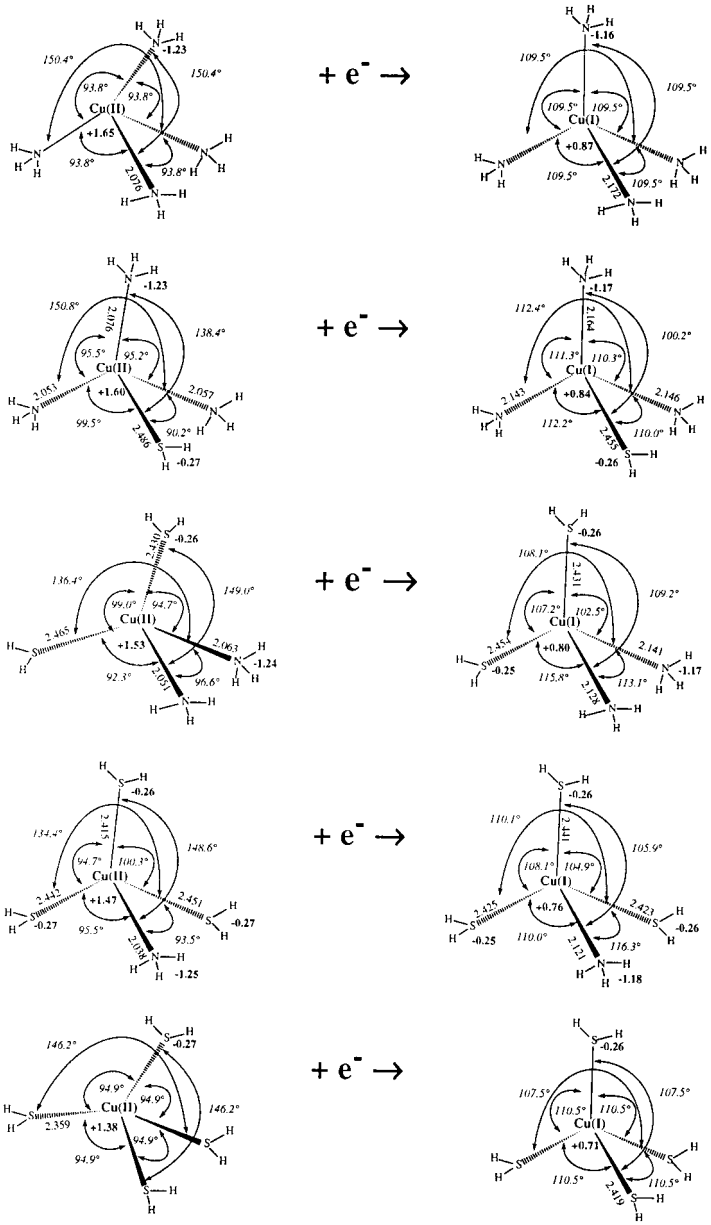

Fig. 7. *Optimized geometries and atomic charges for complex* $Cu^{I}/Cu^{II} \cdot X_mY_n$ (X,Y = NH_3, SH_2; $n+m=4$, $n=0-4$; MP2/LANDL2DZ = *d* optimization, MP2 charges)

population of the Cu 4s orbital (0.11 – 0.15e). The lower positive charge on the Cu^{I} results in less electron density being withdrawn from the liganding atoms, which become less negative. The electron population of the N 2p orbital and of the S 3d orbital

decreases. Finally, the H-atoms attached to the liganding N- or S-atoms become less positive.

A number of geometric consequences accompany the reduction from Cu^{II} to Cu^{I} for all five pairs of complexes. The Cu–X distances increase *ca.* 0.06–0.1 Å. The sum of the six X–Cu–X angles consistently decrease, showing a tendency for the structure to become more tetrahedral in the Cu^{I} oxidation state. As shown in *Table 8*, however, the angular distribution of ligands deviates from regular tetrahedral geometry as a result of the *Jahn–Teller* effect, which is consistent with the results of our CSD study. The deviation from regular tetrahedral geometry given in *Table 8* is found to be larger for the Cu^{II} homoleptic complexes than for the Cu^{II} heteroleptic complexes. This is shown by values of $|\Delta_2|-|\Delta_1|$, where Δ_1 is the deviation from regular tetrahedral geometry of the Cu^{I} complex, and Δ_2 is the deviation from regular tetrahedral geometry of the corresponding Cu^{II} complex for homoleptic systems.

Table 8. *Deviation of the Sum of the Six Bond Angles from Regular Tetrahedral Geometry in Complexes* $Cu^{I}/Cu^{II}\cdot X_nY_m$ (X, Y = NH_3, SH_2, $n+m=4$, $n=0-4$; see *Fig. 7*)

Complex	Deviation from regular tetrahedral geometry [°]		
	Δ_2 [a])	Δ_1 [b])	$\lvert\Delta_2\rvert-\lvert\Delta_1\rvert$
$Cu^{I}/Cu^{II}\cdot(NH_3)_4$	+19.0	0.0	19
$Cu^{I}/Cu^{II}\cdot(NH_3)_3\,SH_2$	+12.6	−0.6	13.2
$Cu^{I}/Cu^{II}\cdot(NH_3)_2\,(SH_2)_2$	+11.0	−1.1	12.1
$Cu^{I}/Cu^{II}\cdot NH_3\,(SH_2)_3$	+10.0	−1.7	11.7
$Cu^{I}/Cu^{II}\cdot(SH_2)_4$	+15.0	0.0	15

[a]) Deviation of $Cu^{II}\cdot X_nY_m$ from regular tetrahedral geometry. [b]) Deviation of $Cu^{I}\cdot X_nY_m$ from regular tetrahedral geometry.

All three heteroleptic systems experience similar deviations from regular tetrahedral geometry, indicating that more than one ligand combination can take part in an electron-transfer process. These findings are supported by a study involving a site mutation in azurin with a change from S to N in the metal coordination. The Met121 residue in the type 1 binding site of azurin was replaced with His at pH 6.5 [63]. As a result, the coordination number of Cu was reduced from 5 to 4, $(His)_3Cys$. A so-called type 1.5 site, *i.e.*, a site which is intermediate between type 1 and type 2, was formed [64]. The optical spectrum of a type 1.5 protein is usually characterized by two intense bands, 580–600 and 430–460 nm. This Met → His mutation did not abolish the Cu-binding properties nor the redox activity of azurin [65].

Binuclear Copper-Binding Motifs in the CSD *and* PDB. Some of the types of motifs found for binuclear Cu complexes in the *CSD* are shown in *Fig. 8*. By far, the most common motif is one in which two Cu-atoms are bridged by two O-atoms. There are fewer structures in which the bridging atoms are N or S. Carboxylate, nitrate, and phosphate groups also act as bridges between the two Cu ions. In most of these complexes in the *CSD*, the Cu···Cu distance does not deviate much from 2.6–2.7 Å.

Discussion. – The aim of this study was to analyze Cu binding patterns in *CSD* and *PDB* data. Several similarities between the two types of molecules have been found.

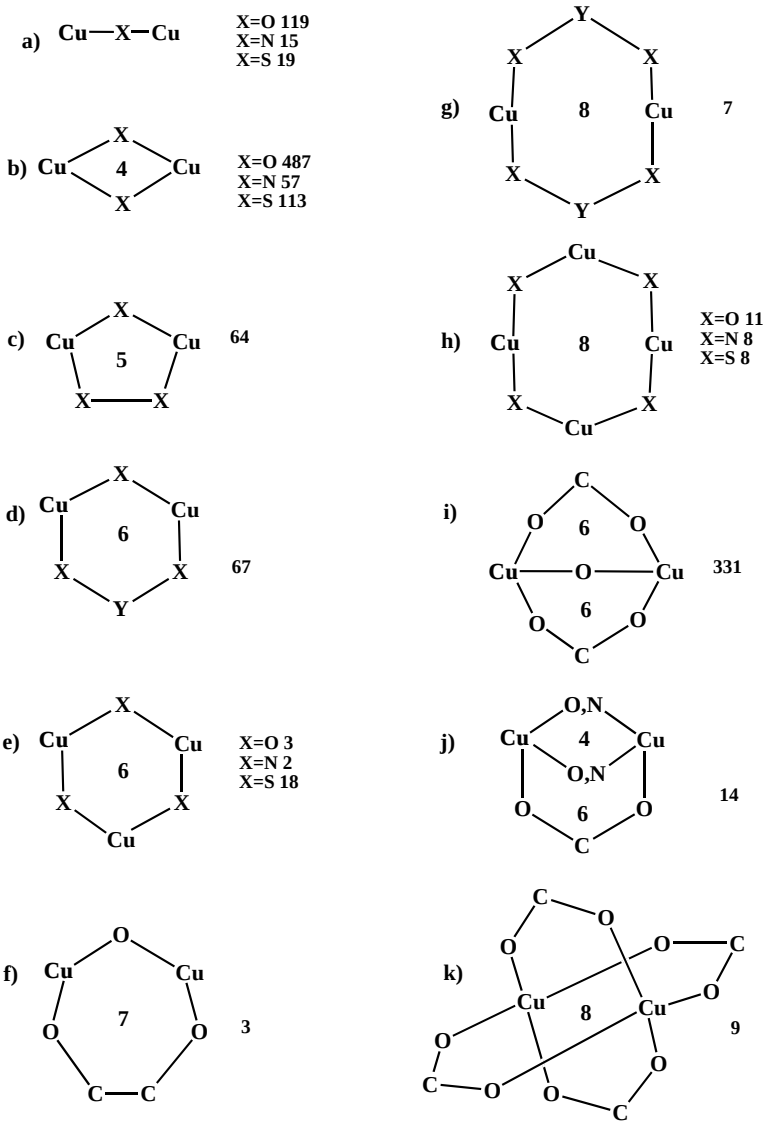

Fig. 8. *Eleven motifs identified in the* CSD *representing some binuclear and trinuclear Cu complexes.* The number of atoms in a cyclic motif is listed within the motif. The number of *CSD* entries with this motif is indicated to the right of the motif.

There is a strong tendency for Cu to form bridged binuclear complexes with O, the system seen in *Fig. 8*, *b*. This motif is also found in some type 3 proteins, such as hemocyanin (see *Fig. 5*). On the other hand, the Cu ions in proteins are nearly always held in place by three (sometimes two) His side chains. In structures found in the *CSD*,

there may not be a sufficient number of N-atoms available to bind the Cu in this way. Therefore O and sometimes S are additionally involved.

The triangular plots shown in *Fig. 2* can now be augmented to include information on proteins, as shown in *Fig. 9*. The electron-transfer enzymes with N_2S_2 or N_2S_2O type 1 binding motifs lie near the sites of 4-coordinate Cu^I. The oxidative enzymes with binding motifs N_2O_3 and N_4O, lie near the sites of Cu^{II}. Cu^{III} is to be found near the apex of the triangle that represents 100% S. The path between Cu^I and Cu^{II} in this diagram (*Fig. 9*) approaches the Cu^{II} site as the coordination number of Cu^I is increased to 5 or 6.

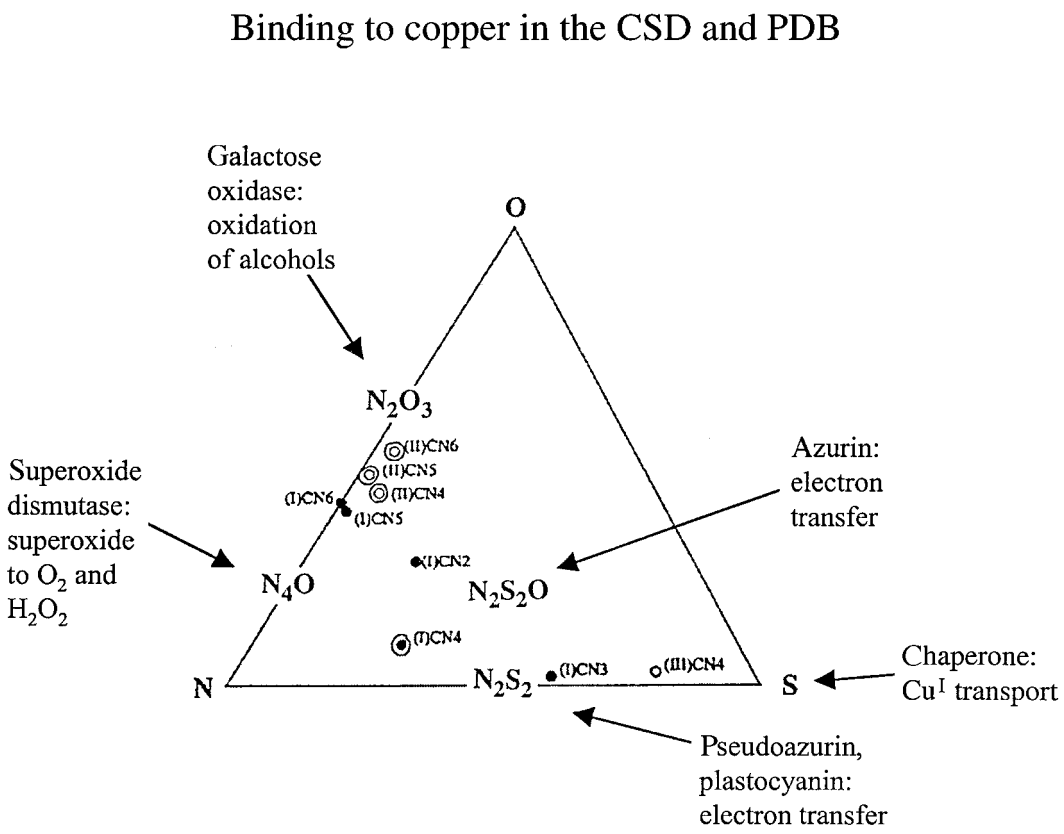

Fig. 9. *Comparison of the information obtained from the* CSD *and* PDB. Cu^I Species represented by filled circles, Cu^{II} and Cu^{III} by open circles; common forms indicated with double circles.

We thank the *Advanced Scientific Computing Laboratory, NCI-FCRF*, for providing time on the CRAY YMP supercomputer. This work was supported by Grants CA10925 and CA06927 from the *National Institutes of Health*, and by an appropriation from the Commonwealth of Pennsylvania. The contents of this article are solely the responsibility of the authors and do not necessarily represent the official view of the *National Cancer Institute*. Part of this work was included in the dissertation of *L. S.-L.* for her Ph.D. degree at the University of Pennsylvania.

REFERENCES

[1] E. J. Underwood, 'Trace Elements in Human and Animal Nutrition', 4th edn., Academic Press, New York, 1977.
[2] E. T. Adman, *Adv. Protein Chem.* **1991**, *42*, 145.
[3] R. A. Pufahl, C. P. Singer, K. L. Peariso, S.-J. Lin, P. J. Schmidt, C. J. Fahrni, V. C. Culotta, J. E. Penner-Hahn, T. V. O' Halloran, *Science* **1997**, *278*, 853.
[4] V. C. Culotta, L. W. Klomp, J. Strain, R. L. Casareno, B. Krems, J. D. Gitlin, *J. Biol. Chem.* **1997**, *272*, 23469.
[5] A. C. Rosenzweig, T. V. O' Halloran, *Curr. Opin. Chem. Biol.* **2000**, *4*, 140.
[6] J. J. R. Fraústo da Silva, R. J. P. Williams, 'The Biological Chemistry of the Elements', Clarendon Press, Oxford, 1991.
[7] B. E. Douglas, D. H. McDaniel, J. J. Alexander, 'Concepts and Models in Inorganic Chemistry', John Wiley, New York 1994.
[8] F. A. Cotton, G. Wilkinson, 'Advanced Inorganic Chemistry: A Comprehensive Text', 4th edn., John Wiley, New York, 1980.
[9] L. E. Orgel, J. D. Dunitz, *Nature* **1957**, *179*, 462.
[10] R. Malkin, B. G. Malmström, *Adv. Enzymol. Relat. Areas Mol. Biol.* **1970**, *33*, 177.
[11] J. A. Guckert, M. D. Lowery, E. I. Solomon, *J. Am. Chem. Soc.* **1995**, *117*, 2817.
[12] M. A. Hitchman, W. Maaskant, J. van der Plas, C. J. Simmons, H. Stratemeier, *J. Am. Chem. Soc.* **1999**, *121*, 1488.
[13] J. A. Fee, *Struct. Bonding* **1975**, *23*, 1.
[14] R. H. Holm, P. Kennepohl, E. I. Solomon, *Chem. Rev.* **1996**, *96*, 2239.
[15] H. Nar, A. Messerschmidt, R. Huber, M. van de Kamp, G. W. Canters, *J. Mol. Biol.* **1991**, *221*, 765.
[16] P. J. Hart, A. M. Nersissian, R. G. Herrmann, R. M. Nalbandyan, J. S. Valentine, D. Eisenberg, *Protein Sci.* **1996**, *5*, 2175.
[17] K. Petratos, Z. Dauter, K. S. Wilson, *Acta Crystallogr.* **1988**, *B44*, 628.
[18] R. L. Walter, S. E. Ealick, A. M. Friedman, R. C. Blake II, P. Proctor, M. Shoham, *J. Mol. Biol.* **1996**, *263*, 730.
[19] J. M. Guss, H. C. Freeman, *J. Mol. Biol.* **1983**, *169*, 521.
[20] L. Chen, R. Durley, B. J. Poliks, K. Hamada, Z. Chen, F. S. Mathews, V. L. Davidson, Y. Satow, E. Huizinga, F. M. D. Vellieux, W. G. J. Hol, *Biochemistry* **1992**, *31*, 4959.
[21] R. Durley, L. Chen, L. W. Lim, F. S. Mathews, V. L. Davidson, *Protein Sci.* **1993**, *2*, 739.
[22] A. G. Sykes, *Adv. Inorg. Chem.* **1991**, *36*, 377.
[23] A. G. Sykes, *Struct. Bonding* **1991**, *75*, 175.
[24] K. Djinovic Carugo, A. Battistoni, M. T. Carri, F. Polticelli, A. Desideri, G. Rotilio, A. Coda, K. S. Wilson, M. Bolognesi, *Acta Crystallogr.* **1996**, *D52*, 176.
[25] N. Ito, S. E. V. Phillips, C. Stevens, Z. B. Ogel, M. J. McPherson, J. N. Keen, K. D. S. Yadav, P. F. Knowles, *Nature* **1991**, *350*, 87.
[26] N. Ito, S. E. V. Phillips, K. D. S. Yadav, P. F. Knowles, *J. Mol. Biol.* **1994**, *238*, 794.
[27] V. Kumar, D. M. Dooley, H. C. Freeman, J. M. Guss, I. Harvey, M. A. McGuirl, M. C. J. Wilce, W. M. Zubak, *Structure* **1996**, *4*, 943.
[28] B. Hazes, K. A. Magnus, C. Bonaventura, J. Bonaventura, Z. Dauter, K. H. Kalk, W. G. Hol, *Protein Sci.* **1993**, *2*, 597.
[29] D. A. Robb, in 'Copper Proteins and Copper Enzymes', Ed. R. Lontie, CRC Press, Boca Raton, Florida, 1984, Vol. II, p. 207 – 240.
[30] R. G. Pearson, *J. Am. Chem. Soc.* **1963**, *85*, 3533.
[31] F. H. Allen, S. Bellard, M. D. Brice, B. A. Cartwright, A. Doubleday, H. Higgs, T. Hummelink, B. G. Hummelink-Peters, O. Kennard, W. D. S. Motherwell, J. R. Rodgers, D. G. Watson, *Acta Crystallogr.* **1979**, *B35*, 2331.
[32] F. C. Bernstein, T. F. Koetzle, G. J. B. Williams, E. F. Meyer Jr., M. D. Brice, J. R. Rodgers, O. Kennard, T. Shimanouchi, M. Tasumi, *J. Mol. Biol.* **1977**, *112*, 535.
[33] J. Erlebacher, H. L. Carrell, ICRVIEW, Program from The Institute for Cancer Research, Fox Chase Cancer Center, Philadelphia, PA, USA, 1992.
[34] M. J. Frisch, G. W. Trucks, H. B, Schlegel, P. M. W. Gill, B. G. Johnson, M. A. Robb, J. R. Cheeseman, T. A. Keith, G. A. Peterson, J. A. Montgomery, K. Raghavachari, M. A. Al-Laham, V. G. Zakrzewski, J. V. Ortiz, J. B. Foresman, J. Cioslowski, B. B. Stefanov, A. Nanayakkara, M. Challacombe, C. Y. Peng, P. Y. Ayala, W.

Chen, M. W. Wong, J. L. Andres, E. S. Replogle, R. Gomperts, R. L. Martin, J. S. Fox, J. S. Binkley, D. J. Defrees, J. Baker, J. P. Stewart, M. Head-Gordon, C. Gonzales, J. A. Pople, GAUSSIAN 94, Gaussian, Inc. Revision A.1, Pittsburgh, PA, 1995.
[35] P. J. Hay, W. R. Wadt, *J. Chem. Phys.* **1985**, *82*, 270.
[36] W. R. Wadt, P. J. Hay, *J. Chem. Phys.* **1985**, *82*, 284.
[37] P. J. Hay, W. R. Wadt, *J. Chem. Phys.* **1985**, *82*, 299.
[38] T. H. Dunning Jr., P. J. Hay, in 'Modern Theoretical Chemistry', Plenum, New York, 1977, p. 1–28.
[39] S. Huzinaga, J. Andzelm, M. Klobukowski, E. Radzio-Andzelm, Y. Sakai, H. Takewaki, in 'Gaussian Basis Sets for Molecular Calculations', Elsevier, New York, 1984.
[40] A. E. Reed, L. A. Curtiss, F. Weinhold, *Chem. Rev.* **1988**, *88*, 899.
[41] F. Weinhold, J. E. Carpenter, in 'The Structure of Small Molecules and Ions', Ed. R. Naaman, Z. Vager, Plenum, New York, 1988, p. 227.
[42] E. D. Glendening, A. E. Reed, J. E. Carpenter, F. Weinhold, 'The NBO 3.0 Program Manual', 1992.
[43] C. W. Bock, A. K. Katz, G. D. Markham, J. P. Glusker, *J. Am. Chem. Soc.* **1999**, *121*, 7360.
[44] A. K. Katz, J. P. Glusker, *Adv. Mol. Struct. Res.* **1998**, *4*, 227.
[45] C. W. Bock, A. Kaufman, J. P. Glusker, *Inorg. Chem.* **1994,** *33,* 419.
[46] J. P. Glusker, *Adv. Protein Chem.* **1991**, *42*, 1.
[47] A. B. Carrell, L. Shimoni, C. J. Carrell, C. W. Bock, P. Murray-Rust, J. P. Glusker, *Receptor* **1993**, *3*, 57.
[48] P. Chakrabarti, *Prot. Eng.* **1990**, *4*, 57.
[49] R. E. Wasylishen, G. Tomlinson, *Can. J. Biochem.* **1977**, *55*, 579.
[50] M. Tanokura, *Biochem. Biophys. Acta* **1983**, *742*, 576.
[51] W. F. Reynolds, I. R. Peat, M. H. Freedman, J. R. Lyerla Jr., *J. Am. Chem. Soc.* **1973**, *95*, 328.
[52] I. Ashikawa, K. Itoh, *Chem. Lett.* **1978**, 681.
[53] E. Vakoufari, K. S. Wilson, K. Petratos, *FEBS Lett.* **1994**, *347*, 203.
[54] J. M. Guss, P. R. Harrowell, M. Murata, V. A. Norris, H. C. Freeman, *J. Mol. Biol.* **1986**, *192*, 361.
[55] W. R. Rypniewski, S. Mangani, B. Bruni, P. L. Orioli, M. Casati, K. S. Wilson, *J. Mol. Biol.* **1995**, *251*, 282.
[56] N. Hakulinen, L.-L. Kiiskinen, K. Kruus, M. Saloheimo, A. Paananen, A. Koivula, J. Rouvinen, *Nat. Struct. Biol.* **2002**, *9*, 601.
[57] A. Messerschmidt, R. Ladenstein, R. Huber, M. Bolognesi, L. Avigliano, R. Petruzzelli, A. Rossi, A. Finazzi-Agro, *J. Mol. Biol.* **1992**, *224*, 179.
[58] A. Kaufman-Katz, J. P. Glusker, G. D. Markham, C. W. Bock, *J. Phys. Chem. B* **1998**, *102*, 6342.
[59] P. George, J. P. Glusker, G. D. Markham, M. Trachtman, C. W. Bock, *Mol. Phys.* (in press).
[60] G. Corongiu, E. Clementi, *J. Chem. Phys.* **1978**, *69*, 4885.
[61] C. W. Bock, M. Trachtman, *Inorg. Chem.* **2002**, *41*, 4680.
[62] M. Trachtman, C. W. Bock, *Inorg. Chem.*, submitted.
[63] A. Messerschmidt, L. Prade, S. J. Kroes, J. Sanders-Loehr, R. Huber, G.W. Canters, *Proc. Natl. Acad. Sci. U.S.A.* **1998**, *95*, 3443.
[64] G. W. Canters, G. Gilardi, *FEBS Lett.* **1993**, *325*, 39.
[65] S. J. Kroes, C. W. G. Hoitink, C. R. Andrew, J. Ai, J. Sanders-Loehr, A. Messerschmidt, W. R. Hagen, G. W. Canters, *Eur. J. Biochem.* **1996**, *240*, 342

Received February 6, 2003